AD-A038 749 GENERAL ELECTRIC CO SANTA BARBARA CALIF DASIAC F/G 7/2
REACTION RATE DATA. NUMBER 57.(U)
AUG 76

UNCLASSIFIED DNA001-75-C-0023
NL

1 OF 1
AD A038749

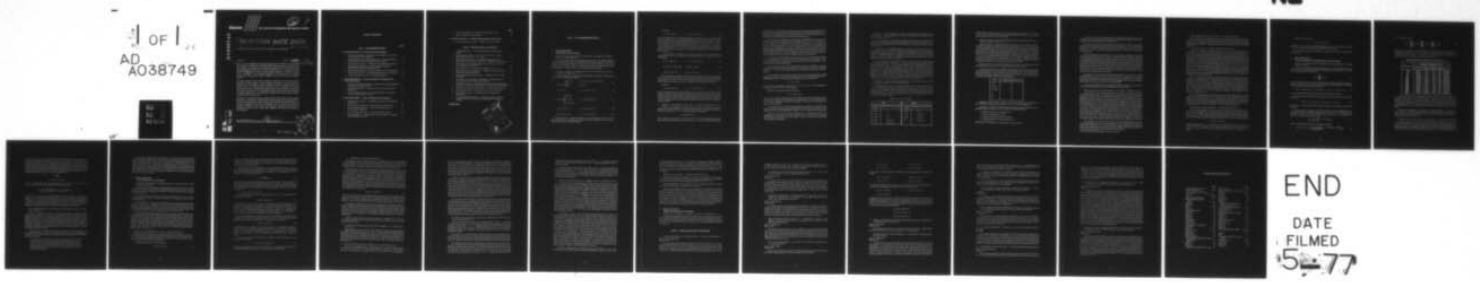

END
DATE FILMED
5-77

(12)

Dasiac **DOD NUCLEAR INFORMATION AND ANALYSIS CENTER**

OPERATED BY TEMPO • GENERAL ELECTRIC COMPANY • FOR THE DEFENSE NUCLEAR AGENCY
816 STATE STREET • SANTA BARBARA • CALIFORNIA 93102 • TELEPHONE (805) 965-0551

(6)

REACTION RATE DATA.

Number 57.

APPROVED FOR PUBLIC RELEASE; DISTRIBUTION UNLIMITED.

Number 57

(11) *Aug[redacted]76*

(12) 24p.

This issue of the DASIAC Reaction Rate Data presents summaries of recent progress for investigations supported by the Defense Nuclear Agency in portions of its Reaction Rate Program, plus summaries of related work submitted by other, non-DNA-funded investigators. Formal DNA reports (where indicated) may be purchased from the Defense Documentation Center, Cameron Station–Building 5, Alexandria, Virginia 22314; alternatively, the information contained in such reports may be obtained subsequently from pertinent articles published in the open scientific and technical journals.

The major portion of this document usually is composed of a number of informal, bimonthly technical progress reports comprising information and data which are considered to be preliminary in nature and may be subject to possible future revision and/or changes. It is requested that recipients do not cite or reference the contents of this issue in other media without receipt of prior specific approval by the author and organization involved. This professional courtesy has been, and will continue to be, greatly appreciated by all contributors, especially those who intend to publish formally elsewhere at a later date.

Submission of subsequent technical progress reports, and/or other pertinent information relevant to those DNA-supported efforts reported herein, deemed appropriate for publication consideration in future editions of the DASIAC Reaction Rate Data are welcome, and should be sent directly to DASIAC, Attn: A. Feryok, General Electric Company–TEMPO, 816 State Street, Santa Barbara, California 93102, which is a DoD-approved activity that is contractually engaged by the Defense Nuclear Agency for this purpose.

(15)

Published for the Defense Nuclear Agency under Contract DNA001-75-C-0023.
This work supported by the Defense Nuclear Agency under: NWED Subtask Code P99QAXDC008, Work Unit 01.

TABLE OF CONTENTS

PART II – ABSTRACTS OF RELEVANT REPORTS

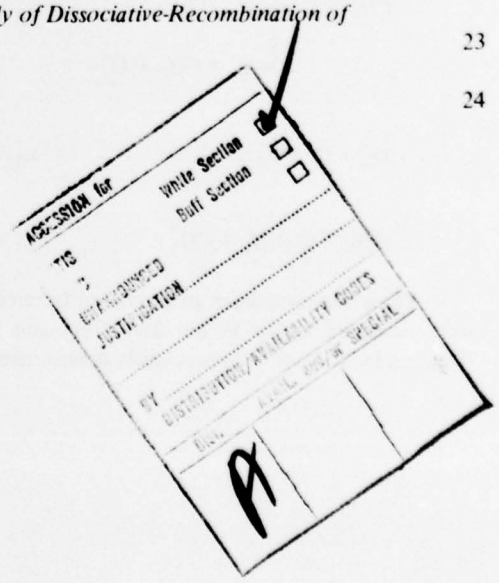

PART I – DNA-SPONSORED RESEARCH

A. Subtask S99QAX HD 010

"Reaction Rates Critical to Propagation"

1. Measurement of Rate Coefficients for Two Body Positive Ion-Negative Ion Neutralization – J. Peterson et al, SRI (Work Unit 69).

The ion optics in the merged beam apparatus have been restored to their original configuration except that the Wien filters are not yet installed, and tests were made on the $O^+ + O^-$ interaction. A signal was observed which appeared to be real; however, the Johnson multiplier used to monitor the neutral product beam was found to be nearly dead, and could only be used as a secondary electron emitting surface. Work is in progress to solve these experimental difficulties.

2. Investigations of Negative Ion Reaction Rates; Effects of Vibrational Excitation Energy – E. Ferguson et al, NOAA (Work Unit 73).

The D-region negative ion chemistry is being reinvestigated and extended. The following reactions with atomic oxygen have been measured:

$$O_2^- + O \xrightarrow{k_{1a}} O^- + O_2 \qquad k_1 = k_{1a} + k_{1b} = 3 \times 10^{-10}\ cm^3\ sec^{-1} \qquad (1)$$

$$O_2^- + O \xrightarrow{k_{1b}} O_3 + e \qquad k_{1a} \cong k_{1b}$$

$$O^- + O \rightarrow O_2 + e \qquad k_2 = 1.9 \times 10^{-10}\ cm^3\ sec^{-1} \qquad (2)$$

$$CO_4^- + O \rightarrow \begin{cases} CO_3^- + O_2 \\ O_3^- + CO_2 \\ O^- + CO_2 + O_2 \end{cases} \qquad k_3 = 2.5 \times 10^{-10}\ cm^3\ sec^{-1} \qquad (3)$$

$$O_3^- + O \rightarrow O_2^- + O_2 \qquad k_4 = 2.5 \times 10^{-10}\ cm^3\ sec^{-1} \qquad (4)$$

$$CO_3^- + O \rightarrow O_2^- + CO_2 \qquad k_5 = 1.1 \times 10^{-10}\ cm^3\ sec^{-1} \qquad (5)$$

These reactions have an estimated uncertainty of ±50 percent. Reactions (1), (2), (3), and (5) were measured earlier in our laboratory and there is satisfactory agreement between the results. Reaction (4) has not been previously determined.

The reaction

$$O_3^- + NO \rightarrow NO_2^- + O_2 \qquad k_6 = 2.9 \times 10^{-12} \text{ cm}^3 \text{ sec}^{-1} \qquad (6)$$

has been investigated in both the flowing afterglow and the flow-drift system and the results obtained in the two systems at thermal energy are in good agreement. The rate constant measured in the flow-drift system is observed to decline initially with increasing ion kinetic energy, reaching a minimum at $KE_{cm} = 0.065$ eV and then it increases rapidly reaching a value of 7.8×10^{-11} cm^3 sec^{-1} at $KE_{cm} = 1.8$ eV. The present result at thermal energy for this reaction is considerably less than an earlier rate constant determination of 1×10^{-11} cm^3 sec^{-1} [Fehsenfeld, Schmeltekopf, Schiff, Ferguson, *Planet. Space Sci.* 15, *373 (1967)*]. Our earlier results were probably influenced by the presence of NO_2 in the NO reactant gas.

A systematic study of atmospheric ions reacting with atomic oxygen and atomic nitrogen is currently being carried out in the thermal energy flowing afterglow. The following reactions have been measured.

$$O_2^+ + N \rightarrow NO^+ + O \qquad k_7 = 1.2 \times 10^{-10} \text{ cm}^3 \text{ sec}^{-1} \qquad (7)$$

$$NO^+ \cdot H_2O + O \rightarrow NO_2^+ + H_2O \qquad k_8 < 10^{-11} \text{ cm}^3 \text{ sec}^{-1} \qquad (8)$$

$$NO_2^+ + O \rightarrow NO^+ + O_2 \qquad k_9 < 10^{-11} \text{ cm}^3 \text{ sec}^{-1} \qquad (9)$$

These reactions have an estimated uncertainty of up to ±50 percent. Reaction (7) was measured earlier in our laboratory. The present result is in satisfactory agreement with this earlier determination, which gave $k = 1.8^{+0.2}_{-0.9} \times 10^{-10}$ cm^3 sec^{-1}. Reaction (7) is important in F-region ion chemistry, while reactions (8) and (9) have been discussed in connection with the D-region ion chemistry.

The reaction

$$CO_3^- + NO \rightarrow NO_2^- + O_2 \qquad k_{10} = 1.1 \times 10^{-11} \text{ cm}^3 \text{ sec}^{-1} \qquad (10)$$

has been investigated in both the flowing afterglow and the flow-drift tube and the results obtained in the two systems at thermal energy are in good agreement. The rate constant measured in the flow-drift tube is observed to decline initially with increasing relative kinetic energy reaching a minimum at $KE_{cm} \cong 0.11$ eV and then to increase, reaching a value of 2.9×10^{-11} cm^3 sec^{-1} at $KE_{cm} = 1.1$ eV. The present results are in good agreement at thermal energy with the earlier determination of the rate constant.

3. Applications of the AIRCHEM Computer Code – J. Heimerl et al, BRL (Work Unit 74).

A version of the AIRCHEM code with a 64 species set and a 495 reaction set has been employed to obtain species densities as a function of time and altitude for the following conditions. The prompt ionization, $N_o = 10^{11}$ cm^{-3}, and the delayed ionization is given by

$$Q(t) = Q_o (1 + t)^{-1.2} \quad ,$$

where t is the time in seconds and $Q = 10^8$ ion-pairs cm^{-3} sec^{-1}. Daytime and nighttime conditions are considered and the calculations correspond to about a 3-hour interval centered around noon and

midnight. Except at 80 km during the night and above 60 km during the day it appears that by 10^4 seconds the electron decay mirrors the production function decay. Three-body attachment is the dominant electron depopulating process at late times except at 70 km and 80 km, and Q is the dominant production mechanism except for late times at 80 km during the day.

Of the 210 ion-ion recombination reactions used in this AIRCHEM code only 8 have been measured in the laboratory. The remaining 202 were assigned a value of $2.0 \times 10^{-7}\ (T/300)^{-.5}\ cm^3\ sec^{-1}$. Since there is some discussion even as to the order of magnitude of some of the measured reactions, computations were made for the two cases wherein all of the ion-ion recombination rate coefficients, α_i's, are multiplied by 10^{-1} and 10^{+1}. Calculations were carried out at 60 km and during nighttime conditions. Results show that though there are large changes in both the total positive ion and total negative ion densities, the change in the electron density barely exceeds a factor of two for a factor of 100 change in α_i. For these circumstances it appears as though it is of the utmost importance to include the correct processes, rather than have very accurate rate coefficients.

The computation of individual species concentrations as a function of time and altitude permits a set of lumped parameters to be generated. Of those computed the most interesting are: (1) the effective electron-ion rate coefficient, α_d, (2) the effective electron detachment frequency, D, and (3) the effective recombination coefficient, ψ.

For the lower altitudes ($Z \leqslant 50$ km) α_d approaches limiting values determined by the relative composition of cluster ions and their respective electron-ion recombination coefficients. At the higher altitudes ($80 \leqslant Z \leqslant 60$ km) computed α_d's did not attain their limiting values even after 10^4 model seconds.

The most notable feature observed in curves of D versus t is that no curve attains a constant value at late times (10^4 sec). However, some caution must be exercised. Preliminary analysis of the AIRCHEM output shows that a detachment process which is important at all altitudes is

$$O^- + N_2 \rightarrow N_2O + e \ .$$

The reaction has been assigned the upper limit of $1 \times 10^{-12}\ cm^3\ sec^{-1}$ and the consequences of varying this value have not yet been fully investigated.

The effective recombination coefficient is defined by

$$\psi = (1 + \lambda)(\alpha_d + \lambda\alpha_i) \ ,$$

where λ is the ratio of the total negative ion density to the electron density, and α_i here is the effective ion-ion rate coefficient. In the steady state, ψ should equal the source term divided by the electron density squared, Q/E^2. We find that ψ and Q/E^2 are about equal for times greater than about 1 second, for all cases.

At an altitude of 60 km for both daytime and nighttime conditions, our computed electron density, total positive ion and total negative ion densities as a function of time are in good-to-excellent agreement with the corresponding densities of Scheibe. A report is being prepared on these results.

In order to study less severe ionization conditions, source routines are being added to the AIRCHEM program. The sources of ionization added are due to: (1) solar photons, (2) secondary photoelectrons, and (3) galactic cosmic rays. A report on sources of ionization in the mesosphere and stratosphere is being prepared.

A six-ion code, similar to that described by Mitra, was assembled and made operational. The six species are O_2^+, O_4^+, NO^+, $H^+(H_2O)_n$, e, O_2^- and X^-. Difficulties remain in the definition of the electron detachment rate of X^-.

An invited paper entitled "Modeling of Charged Particle Chemistry in the Stratosphere and Mesosphere" was presented at the Spring Annual Meeting of the AGU. This talk included a discussion of results from AIRCHEM and from the six-ion model for quiet, midlatitude equinox conditions at 1330 local time.

For positive ions, the AIRCHEM computations showed that between 80 and 90 km NO^+ is the dominant ion while below 70 km (down to 20 km) the hydrated protons are dominant. The level of hydration is mainly controlled by the temperature profile employed. In contrast to the positive profiles, the AIRCHEM computations for negative ions showed that the identity of the dominant negative ion changes with altitude. This suggests that characterization of the negative ions by a single species, X^-, in the six-ion code, may be too simple.

Computed total positive ion profiles (20 to 90 km) compare well with each other and with the conductivity measurements of Mitchell (30 to 75 km). These measurements were made at White Sands Missile Range 1 Feb 71, 1315 LT. Only fair agreement between AIRCHEM and the six-ion codes was obtained for the electron profile below ~50 km. Above this altitude the codes agree to within a factor of three suggesting the difference lies in the handling of the negative ions. Both code results agree with the Illinois measurements (Wallops Island, 31 Jan 72) also taken during a "quiet" period. These experimental results extend from 50 to 80 km. On the other hand, the shape of the measured electron profile of Mitchell is difficult to reconcile with either of the model results. Mitchell's results extend from 40 to 65 km. However, these blunt probe measurements are being reanalyzed taking into account aerodynamic effects on the velocity determinations.

The negative ion computed results show that between ~55 and 70 km negative ion photodestruction, while not dominant, cannot be completely neglected.

The AIRCHEM code, tailored for quiet conditions, has been run for Wallops Island, Virginia, 31 Jan 72. Charged particle profiles were computed at 5-km intervals from 90 to 20 km for both near-noon and near-midnight conditions. The predicted dominant negative ions are shown in the accompanying table. The most obvious feature seen in the table is the dramatic change in negative ion composition from day to night. Code predictions also show that for altitudes above about 75 km the path for the formation of H_3O^+ is

$$NO^+(H_2O)_2 + h\nu \rightarrow H_3O^+ + HNO_2 \quad .$$

DAY		NIGHT	
ALTITUDE (km)	DOMINANT NEGATIVE ION	ALTITUDE (km)	DOMINANT NEGATIVE ION
90-85	O^-	90-80	NO_3^-
80-70	O_2^-	75-65	$NO_3^-(H_2O)$
65-55	CO_3^-	60-25	$CO_3^-(H_2O)$
50-35	$NO_3^-(H_2O)$	20	$CO_4^-(H_2O)$
30-20	$NO_3^-(HNO_3)$		

when an assumed cross section of 10^{-18} cm^2 is used across the solar spectrum, $125 < \lambda < 730$ nm. A six-ion code is presently being developed from the multispecies code results to cover the entire altitude range from 20 to 90 km for quiet conditions.

4. *Positive and Negative Ion Reactions, Photodissociation Reactions Hindering Cluster Ions – J.A. Vanderhoff et al, BRL (Work Unit 75).*

We have continued to investigate the photodissociation cross sections for $O_2^+(O_2)$, $O_2(H_2O)_{1,2}$, and $O_2^+(CO_2)$. During this reporting period the photon energy range from 1.952 to 2.254 eV has been covered by using Rhodamine 6G and 110 dyes in a tunable dye laser. The measured photodissociation cross sections fitted smoothly into the cross sections obtained from the discrete lines of the argon and krypton ion lasers. A threshold (within experimental uncertainty $\sim 1 \times 10^{-19}$ cm^2) of ~2.02 eV was observed for the onset of photodissociation for $O_2^+(CO_2)$. The appearance of the CO_2^+ photofragment at ~2.16 eV from the photodissociation of $O_2^+(CO_2)$ can be used to place an upper limit on the dissociation energy of $O_2^+(CO_2)$. That is, $D[O_2^+(CO_2)] \leq 2.16$ eV $- [IP(CO_2) - IP(O_2)]$, where IP stands for ionization potential. Using 13.769 eV and 12.063 eV as the ionization potentials of CO_2 and O_2, respectively, an upper limit for the dissociation energy is placed at 0.46 eV.

Recently, positive ion clusters have been produced in CO_2 gas by electron impact and a large photodissociation cross section ($\sim 10^{-18}$ cm^2) was observed for $C_2O_4^+$ at 2.540 eV.

A new krypton ion laser has been operated in the all-lines UV* region to obtain photodestruction cross-section values for various atmospheric ions. Preliminary values for these cross sections are listed in the table below. To place these cross sections on an absolute scale we normalized to the previously measured photodetachment cross section for O_2^- (3.5×10^{-18} cm^2). The drift tube region was operated at an E/N of 15 Td for all of these measurements.

ION	CROSS SECTION (10^{-18} cm^2)
$O_2^+(O_2)$	2.9
$O_2^+(H_2O)$	11.0
$H_3O^+(OH)$	3.4
O^-	8.3
NO_2^-	4.9
O_3^-	1.2

Investigations have just started for positive ions of nitric oxide. The dimer, $NO^+(NO)$ was found to exhibit an extremely large cross section ($\sim 2 \times 10^{-17}$ cm^2) in the 6000A region.

CO_2 Negative-Ion Studies. Experimental work on this project is tentatively believed to be completed. Reaction rate coefficients at $20 < E/N < 300$ Td have been established for:

- Dissociative attachment of electrons to CO_2
- Three-body attachment of O^- to CO_2
- Collisional dissociation of CO_3^- into O^- and CO_2
- Collisional detachment of electrons from O^- in CO_2.

*The composition of the UV light is about 74 percent 3507A and 26 percent 3564A.

A first draft of a report for publication has been completed. Final completion awaits analysis of arrival-time spectra using the Gatland-Colonna-Romano-Keller procedure extended to include three source-generated components (electrons, O^- and CO_3^- ions).

Na^+ Cluster-Ion Studies. The drift tube-mass spectrometer has been utilized to study positive sodium ions in N_2 and O_2 gases. The drift distance has been lengthened to 8.87 cm and a hot-filament alkali ion source installed. In addition to the parent Na^+ ion, the clusters $Na^+ \cdot O_2$ in O_2 and $Na^+ \cdot N_2$ and $Na^+ \cdot 2N_2$ in N_2 have been observed. Preliminary analysis of arrival-time spectra at low E/N (<24 Td) has begun.

Drift-Tube Mass-Spectrometer Experiment. A new technique for analyzing the negative-ion reactions in CO_2 has been developed. It consists of applying a very high stopping (or bias) voltage to the Tyndall double grid gate so that electrons as well as negative ions are stopped, followed by a correspondingly high pulse of voltage to open the gate for a few microseconds. By this procedure the electrons as well as the negative ions are gated, in contrast to the previous practice both here and elsewhere that lets electrons leak continuously through the gate. The result of the new technique is that the arrival time spectra are *much* richer in information concerning reactions and reaction rates. The data are put into a new computer program geared to analyze three incident ions (electrons, O^-, and CO_3^-) and five ensuing reactions. Not only are more consistent data being obtained, but more total data on the various reaction rate coefficients.

The positive ions in CH_4 have been examined experimentally with the objective of finding an E/N dependence of the reaction $CH_4^+ + CH_4 \rightarrow CH_5^+ + CH_3$. The reaction proved to be so rapid that it went to completion in the relatively long drift distances of our apparatus. It could only conceivably be done with the aid of a dilutant gas for which the apparatus is not at the moment equipped. There was also concern as to the purity of the CH_4 supply available.

A return was accordingly made to the incompleted cluster-ion experiments of Na^+ with various atomic and molecular gases. This project has just been begun in the report period.

5. Chemistry and Spectroscopy of Optical Emitters – D.E. Snider et al, BRL (Work Unit 76).*

Line parameters for three vibration-rotation bands of NO_2 and for three bands of SO_2 have been generated and compiled on a computer tape with the same format as the AFGL line parameters tape. The three bands for NO_2 are the (010), the (001), and the (101). Line positions for the two fundamentals have been computed from recent work of Cabana *et al* which includes effects of spin splitting. Line positions for the (101) combination band were computed from constants given by Olman and Hause. The total band strength for (001) given by Goldman *et al* was used to normalize the computed lines. For the (101) combination band, the band strength given by Guttman was used. For the (010) fundamental, an estimated band strength given by Hurlock *et al* was used. Halfwidths computed by Tejwani were assumed. The same three bands for SO_2 were also computed. Relative line positions for the (010) and the (001) fundamental bands were computed from rotational constants measured by Steenbeckeliers in the microwave region. The band centers for (001) given by Dana and Fontanella and for (010) given by Cordice *et al* were used to obtain absolute line positions. Line positions for the (101) combination band were computed from the constants of Barbe *et al*. For all of the SO_2 bands an average air-broadened halfwidth given by Hinkley *et al* was assumed, and weighted average band strengths given by Young *et al* were used to normalize the line intensities.

The COSMEP IV series with four balloon flights was held during April/May 1976 near Fairbanks, Alaska. Excellent IR emission and transmission spectra were obtained and the data are being analyzed. Three flights were flown to study the temporal, spatial, and spectral nature of enhanced infrared background emissions in the northern latitudes. One flight was devoted to the study of the infrared transmission properties of the stratosphere for long optical paths.

*Now at the Atmospheric Science Laboratory, White Sands Missile Range.

6. *Improved Master/Simple Codes for E-, F-Regions – W. Ali, NRL (Work Unit 77)*

During this period a comprehensive set of charge exchange and rearrangement processes in disturbed E- and F-regions were compiled. These reactions were described in a report for their implications in terms of deionization and emission. Many of the reactions involved are not well known. A simple approach is devised to account for these reactions and are being incorporated into the NRL Master Code.

7. *Ion-Neutral Investigations – E. Murad, J. Paulson, AFGL (Work Unit 78).*

Studies were continued on collisional dissociation and other reactions of terminal negative ions. Observations made at SRI on the photodissociation of CO_3^- led us to study the reaction $CO_3^- + O_2 \rightarrow O_3^- + CO_2$. From drift tube afterglow studies at NOAA, this reaction is known to be slow in the direction written but fast in the reverse direction at thermal and near-thermal energies. However, the photodissociation studies indicated similar thresholds for photodissociation of CO_3^- and of O_3^-, suggesting that the reaction is approximately isoergic. Our cross sections for the forward reaction show an onset at about 3 eV in the lab coordinate frame, rising to a value of 0.6×10^{-16} cm^2 at 15 eV (lab). Cross sections for the collisional dissociation reaction channel, $CO_3^- + O_2 \rightarrow O^- + CO_2 + O_2$, show an onset at approximately 5 eV (lab) but climb to a value of 5×10^{-16} cm^2 at 15 eV and to 26×10^{-16} cm^2 at 50 eV. Thresholds for these reactions are not well defined, in part because of the presence of excited states of CO_3^- in the beam. However, the results are of interest in showing both the occurrence of the ion transfer reaction, leading to O_3^- production, and the occurrence of collisional dissociation with cross sections significantly larger than those for the ion transfer process through most of the energy range studied.

Work was continued on positive ion photodissociation reactions. Our apparatus permits absolute cross-section measurements with a wavelength resolution of 0.1 nm. Cross sections have been measured for H_2^+ and D_2^+ in order to compare with previous measurements, which were made at a bandwidth of 20 nm. The results agree to within 10 percent. With the use of time-of-flight measurements we have been able to identify the vibrational levels of the dissociating state. Cross sections have recently been measured for N_2O^+ photodissociating to NO^+ and N in the wavelength range from 300 to 330 nm. A peak in the absorption cross section is observed at 322 nm with a half-width of 2 nm. No dissociation to $O^+ + N_2$ could be observed. Attempts to observe photodissociation of NO_2^+ have so far been unsuccessful.

The AFGL high-temperature mass spectrometer was assembled and adjusted and a mass resolution of about 600 has been achieved so far. It is expected to obtain a resolution of 1500 shortly. Attempts to study the reactions of UO^+ with O_2 have proved unsuccessful due to the poor mass resolution of the primary mass analyzer in the double mass spectrometer system. A contract has now been written with the University of Pittsburgh to measure these reactions and their rate constants. It is expected that work on the reaction $N^+(^3P) + O_2 \rightarrow NO^+ + O(^1S)$ will begin soon.

Thermochemistry of Gaseous Metal Oxides – D.L. Hildenbrand, SRI (Work Unit 78)

Gaseous reaction equilibria in the U-Ti-O system were studied in detail during this period in order to resolve conflicting data on U-O bond dissociation energies. The reactions were studied in the range 2150 to 2300K by high-temperature mass spectrometry. Because of major uncertainties in the spectroscopic and molecular constants of the gaseous uranium oxides, the thermochemical data were derived solely from a second law analysis of the equilibrium data. For the gaseous reaction

$$Ti + UO_3 = TiO + UO_2$$

the enthalpy change $\Delta H_o^\circ = -12.3 \pm 2.4$ kcal/mol was obtained, leading to $D_o(O_2U\text{-}O) = 146.1$ kcal (6.34 eV). This is in close agreement with our earlier value $D_o(O_2U\text{-}O) = 145.4$ kcal (6.30 eV) obtained from studies of the U-Al-O system, indicating that $D_o(O_2U\text{-}O)$ can be considered as well defined.

Similar studies of the reaction

$$Ti + UO_2 = TiO + UO$$

yielded $\Delta H_o^\circ = 18.2 \pm 3.0$ kcal/mol and $D_o(UO\text{-}O) = 176.6$ kcal (7.66 eV). Further studies under more reducing conditions will be required to define $D_o^\circ(UO)$ in the same way.

Some additional measurements of $IP(UO_3)$ are being carried out and will be completed during the next period.

B. Subtask S99QAX HD 028

"Theoretical Investigations of Ionizing Mechanisms in the Upper Atmosphere"

1. Computations of Structure and Transition Probabilities in Atmospheric Molecules – H. Michels, UARL (Work Unit 37).

An analysis of all available experimental and theoretical data relating to the dipole moment of NO was carried out. All data, including experimental integrated absorption coefficients, were reduced to fit a dipole moment function of the form:

$$\mu(r) = \sum_{j=0}^{4} a_j (r-r_e)^j \qquad (1)$$

A computer reduction was carried out using a least-squares fit to all data weighted by the given error analysis (or estimated errors in the case of the calculated dipole moment functions). A minimum error residual was found with the following function:

$$\mu^{NO}(r) = -0.166 + 2.24\,(r-r_e) - 1.342\,(r-r_e)^2 - 1.703\,(r-r_e)^3 + 1.097\,(r-r_e)^4 \qquad (2)$$

where r_e is the equilibrium internuclear separation in angstroms and $\mu(r)$ is in Debyes.

This function can be compared with the "experimental" dipole moment function for CO found by Toth *et al*

$$\mu^{CO}(r) = -0.112 + 3.10\,(r-r_e) - 0.31\,(r-r_e)^2 - 2.28\,(r-r_e)^3 \qquad (3)$$

The functions are clearly similar both with regard to the sign of the coefficients and their relative magnitudes.

Using the dipole moment function represented by Equation (2) and accurate RKR vibrational-rotational wavefunctions, the integrated band absorption coefficients have been calculated for the fundamental, first, and second overtones of NO as a function of temperature. For a transition from lower state ℓ to upper state u in absorption we have

$$S_{\ell u} = \frac{\pi e^2}{mc^2}\,\frac{N_\ell}{P}\left[1 - e^{-hc\nu_{\ell u}/kT}\right] f_{\ell u} \qquad (4)$$

where $f_{\ell u}$ is the absorption f-number. In computational form we have

$$S_{\ell u}(T) = 2.3795 \times 10^7 \left(\frac{273.16}{T(K^\circ)}\right)\left(\frac{N_\ell}{N_T}\right)\left[1 - e^{-1.4388\,\nu_{\ell u}(cm^{-1})/T(K^\circ)}\right] f_{\ell u} \qquad (5)$$

The total absorption is given by

$$S(T) = \sum_{\substack{\ell=0 \\ u=\ell+1}} S_{\ell u}(T) + \sum_{\substack{\ell=0 \\ u=\ell+2}} S_{\ell u}(T) + \sum_{\substack{\ell=0 \\ u=\ell+3}} S_{\ell u}(T) + \ldots \qquad (6)$$

where the first term represents the total absorption of the fundamental band, the second term represents the first overtone absorption, etc. The calculated absorption is given in the accompanying table which indicates a near constancy of the intensity of the fundamental band up to 5000K. This is in agreement with the recent experimental data of Konkov and Vorontsov.

Total Integrated Absorption Coefficients for Nitric Oxide ($X\ ^2\Pi$)

Temperature (K)	Absorption Coefficient, $cm^{-2}\ atm^{-1}$				
	Fundamental	First Overtone	Second Overtone	Third Overtone	Total
100.	122.642	2.127	.031	.000	124.800
273.16	122.641	2.127	.031	.000	124.799
300.	122.640	2.128	.031	.000	124.799
500.	122.606	2.147	.032	.000	124.785
1000.	122.069	2.433	.038	.000	124.540
1500.	121.032	2.967	.053	.000	124.052
2000.	119.775	3.618	.075	.000	123.468
2500.	118.402	4.231	.106	.001	122.740
3000.	116.953	5.065	.146	.004	122.168
4000.	113.916	6.591	.254	.009	120.770
5000.	108.614	8.123	.360	.021	117.118
8000.	100.382	12.030	.882	.061	113.355
10000.	93.232	13.662	1.154	.087	108.135

A systematic study of the computational model of the multiple-scattering X_α formalism was undertaken. This included an examination of the choice of size of sphere radii in the muffin-tin approximation and the choice of the exchange parameter, α. We find a variational minimum in the total X_α energy for sphere radii which yield a uniform value for the spherically averaged potential at each sphere boundary. The total energy is sensitive to the choice of sphere radii and we find optimum wavefunctions only when the sphere radii are adjusted to variationally yield a minimum total energy.

In addition, we find improved total energies if the exchange parameter, α, for each atom is varied to account for the different degree of ionicity on each atomic center as a function of interatomic separations. This dynamic exchange scaling has not been attempted before but appears to yield much more reliable total energies.

2. Theoretical Aspects of SRI Laboratory Ion-Ion Measurements–F. Smith, SRI (Work Unit 39).

To quantify the role of energy transfer to internal modes of a molecular ion as the first step in the ion-ion recombination process, we have continued to develop the general calculational procedure through the use of a simple model problem, the rotational excitation of a polar diatomic ion (or neutral molecule). A brief paper has been written, "Test of Semiclassical Perturbation Scattering Theory: Collisions of Electrons with Rotating Dipole Molecules," by F.T. Smith, D. Mukherjee, and

D.L. Huestis, representing recent work on this problem. It also incorporates work carried out under other sponsorship (chiefly AFOSR) related specifically to the problem of electron collisions with neutral polar molecules such as the alkali halides. The general procedures for obtaining total cross sections from the scattering matrix are important for future applications to the ion-ion neutralization problem. We have developed efficient and reliable integration procedures to carry out the complex summations that enter into the problem. We have now shown that the final rotational excitation cross sections for the case where electrons or ions collide with neutral polar targets depend inversely on the collision and directly on a function of only two reduced parameters,

$$\beta = \frac{m\mu e}{\hbar^2} \quad ,$$

$$g = (2j+1)_\alpha = (2j+1)\hbar^2/2IE \quad ,$$

where μ is the dipole moment, I is the moment of intertia, n is the reduced mass, E is the energy, and $j = j_1 + \frac{1}{2}\Delta j$ is the average of initial and final rotational quantum numbers:

$$\sigma_{\Delta j} = \frac{\pi\hbar^2}{2mE} \frac{2j+1}{2j_1+1} \left[n^{(0)}_{|\Delta j|}(\beta^2, g) + \frac{1}{(2j+1)^2} n^{(1)}_{|\Delta j|}(\beta^2, g) + \ldots \right]$$

The second term in the expansion is usually negligible, except for very small j ($j \lesssim 5$). The functions $n_{|\Delta j|}(\beta^2, g)$ can be generated and tabulated, and used for the rapid estimation of any needed rotational excitation cross section for polar molecular targets. Now that we understand the general form of solution, we can develop analogous expressions for the ion-dipole ion problem. Furthermore, by summing over an appropriate range of the parameter Δj, we can generate a reduced form of the expression that is needed to obtain capture cross sections and to estimate neutralization rates.

3. *Investigations Relevant to the "Twilight Anomaly" and Other Relevant Problems – W. Swider, AFGL (Work Unit 39).*

Estimates of photodetachment rates for various important negative ions were placed in the Keneshea Code. Computer runs were made for the disturbed D-region. Best comparison with disturbed D-region daytime data was attained when rather high cross sections were adopted for photodetachment processes, i.e., cross sections approaching about the maximum possible, near 100 Mb. However, agreement with the twilight data was poor because the effective wavelengths for the photodetachment processes were uncertain and hence the appropriate twilight attenuation conditions for the incident wavelengths. It would appear that there remain too many unknown reaction rates (particularly for negative ions), photodetachment rates, etc., for an empirical approach to the solution of the twilight anomaly problem.

During this period, we collaborated with Dr. Narcisi concerning a steady-state analysis of the ion composition data taken on 27 March 1973 at Poker Flat, Alaska, as part of the ICECAP program. A paper was prepared concerning the analysis and submitted to the *Journal of Geophysical Research*. The abstract is as follows:

> Good agreement is obtained between the calculated and observed O^+, N_2^+ and N^+ ion distributions for an aurora with a peak electron concentration of about 1.1×10^6 cm^{-3} near 110 km. The NO profile required to explain the NO^+ and O_2^+ data is deduced and discussed. The inferred peak nitric oxide concentration is among the three largest (all about 10^9 cm^{-3}) values ever derived in studies of over a dozen AFGL auroral rocket flights.

A meeting was attended at Palo Alto, California on 16-20 Feb 1976 concerning Lockheed's assessment of the Aug 1972 SPE. The results for this event paralleled the information obtained from the Nov 1969 SPE, in general, except that for the Aug 1972 case, a higher daytime electron loss factor was ascertained for 80 km, possibly because of especially cold mesopause temperatures. Fortunately, this altitude has only a small impact on HF/VHF absorption or LF/VLF propagation (for disturbed conditions). Lockeed's report contained considerable twilight data which should contribute to the twilight anomaly studies. However, the rate of change of the solar zenith angle varies at twilight as a function of season. Hence, twilight anomaly studies must be cautious in matching calculations with data from only one season.

C. Subtask S99QAX HI 002

"Atomic and Molecular Physics of IR Emissions"

1. Fine Definition of IR Spectra for Certain Metal Oxide Species – D.W. Green, Argonne National Laboratory (Work Unit 28).

An article entitled, "Infrared Spectra of Matrix-Isolated UO_2^+ and NO_2^-," has been published. In this work the only cation identified was UO_2^+ although the production of UO^+ was also thermodynamically favorable. In a further attempt to produce the UO^+ cation, U atoms have been cocondensed in an Ar matrix with NO_2.

The occurrence of the neutral reactions, $U + NO_2 \rightarrow UO + NO$ and $U + NO_2 \rightarrow UO_2 + N$, has been confirmed by the observation of the known $U^{18}O$ and $U^{18}O_2$ frequencies from the reactions of ^{18}O-enriched NO_2.

In the 1250-1200 cm^{-1} range, peaks were observed at the same frequencies as peaks previously assigned by others to "free" or "isolated" $N^{16}O_2^-$, $N^{16}O^{18}O^-$ and $N^{18}O_2^-$. Small amounts of UO_2^+ isotopomers were also present. In addition, ^{15}N has been used to identify the absorbers responsible for some previously unidentified peaks, namely, UN, tentatively UN_2 and a species labeled X-UN which contains one nitrogen atom and no oxygen atoms but is not the diatomic UN.

Several experiments have been completed in which U atoms were cocondensed with 1 percent or 0.1 percent NO_2 in Ar. Pure $N^{16}O_2$, 50 percent ^{18}O-enriched and 90 percent ^{18}O-enriched NO_2 have all been used. A number of weak peaks have been observed in these experiments but no assignment to the UO^+ cation has yet been possible. The absorbers responsible for the large number of unlabeled weak peaks remains unknown. However, it does appear that UO^+ is not present in a sufficient concentration to give an observable spectrum. We tentatively conclude that the reaction $U + NO_2 \rightarrow UO^+ \cdot NO^-$ does not compete favorably with other reactions. Further experiments are planned with U + NO, UO + I and Th + NO_2 as well as further attempts to identify additional products of the U + NO_2 reaction.

2. Reactions between AlO and O Atoms – A. Fontijn, AeroChem (Work Unit 29).

In previous work we obtained the rate coefficients of the Al/O_2 and AlO/O_2 reactions in the 300-1700K range in high-temperature fast-flow reactors (HTFFR). Since the fate of gaseous AlO_x (x = 1,2) and its effects in disturbed atmospheres can also depend on its reactions with O atoms we are obtaining kinetic information on these reactions.

To calculate an upper limit for the rate coefficient of

$$AlO + O \rightarrow Al + O_2 \qquad (1)$$

a study of the $A\ell/SO_2$ reaction is being made to determine a lower limit for $D(A\ell-O)$ and hence a lower limit to the activation energy, E_A, of Reaction (1). Preliminary data suggest $D(A\ell-O) \geq 128$ kcal mole^{-1} and hence E_A for Reaction (1) is ≥ 10 kcal mole^{-1}, making it essentially an infinitely slow process at temperatures of interest.

The mechanism of the chemiluminescence emitted in $A\ell/A\ell O/O/O_2$ systems is being investigated. Insufficient data have been obtained thus far to establish the reaction mechanism. A comparison to the O/NO glow intensity suggests, based on initial [$A\ell$], a rate coefficient $k_{h\nu}$ of $\approx 10^{-13}$ ml molecule^{-1} sec^{-1} for the "formal" reaction

$$A\ell + O \xrightarrow{(M)} A\ell O + h\nu \qquad (2)$$

This value for $k_{h\nu}$ is *(i)* in good agreement with Golomb and Brown's value for the rate coefficient for light emission from the O + trimethylaluminum reaction, *(ii)* so high as to make Reaction (2), as written, an improbable mechanism, and *(iii)* sufficiently fast to suggest that the reactions leading to the chemiluminescence may be important in determining $A\ell O_x$ concentrations in disturbed atmospheres.

a. Kinetics of $A\ell O + O \xrightarrow{(1)} A\ell + O_2$

Presently accepted values for $D(A\ell-O)$ range from 120-122.5 kcal mole^{-1}. Recently the activation energy for the reaction

$$A\ell + CO_2 \rightarrow A\ell O + CO \qquad (3)$$

was measured to be ≤ 3.3 kcal mole^{-1}. Since $E_A \geq \Delta H$, this activation energy would only be compatible with the lower limit to its ΔH and hence with the upper limit value for $D(A\ell-O)$ of 122.5 kcal mole^{-1}. Consequently, since $D(O-O) = 118$ kcal mole^{-1}, Reaction (1) is at least 4.5 kcal mole^{-1} endothermic. Recalculating the equilibrium constant for Reaction (1) by using $D(A\ell-O) = 122.5$ kcal mole^{-1} to correct the JANAF tables data yields K_1 (300K) $= 5.2 \times 10^3$. Since $k_{-1} = (3 \pm 2) \times 10^{-11}$ ml molecule^{-1} sec^{-1}, k_1 (300K) $\leq 1 \times 10^{-14}$ ml molecule^{-1} sec^{-1}.

We obtained indications from the study of the $A\ell/SO_2$ and $A\ell$/NO reaction that $D(A\ell-O)$ may be higher yet and consequently that the upper limit to k_1 is even lower. We are currently investigating these reactions further to settle this point. A set of measurements of the reaction

$$A\ell + SO_2 \rightarrow A\ell O + SO \qquad (4)$$

at 700K indicates a rate coefficient of 6×10^{-12} ml molecule^{-1} sec^{-1} independent of pressure between 3 and 10 Torr. If we assume a pre-exponential for this reaction of 3×10^{-10} (i.e., gas kinetic) then its $E_A = 1.4$ kcal mole^{-1}. Since $D(O-SO) = 131.6 \pm 2$, the indicated $D(A\ell-O)$ is ≥ 128 kcal mole^{-1}. A direct measurement of this E_A by extending the k_4 measurements down to $\approx$300K is now needed.

A series of measurements in the $A\ell$/NO system at 600K showed $A\ell$ consumption to occur via a three-body reaction, hence

$$A\ell + NO + M \rightarrow A\ell NO + M \qquad (5)$$

with a rate coefficient of $(2 \pm 1) \times 10^{-31}$ ml^2 molecule^{-2} sec^{-1}. Since this type of reaction cannot give information on $D(A\ell-O)$ and hence k_1, this study will not be pursued further.

b. Chemiluminescence in the Aℓ/AℓO/O/O_2 System

The apparatus used in this phase of the work is a modified version of the "300 K" HTFFR described previously. An inlet for introduction of O atoms has been added 2.5 cm upstream from the observation window. O atoms are produced by NO titration of N atoms produced in a microwave discharge through N_2. Upstream from this inlet, O_2 can be introduced to convert Aℓ to AℓO.

The Aℓ-oxidation continuum was observed in the reaction between Aℓ and O atoms at 2 and 5 Torr and will, for short, be referred to as the Aℓ/O glow. The intensity of the glow varies as $[A\ell]^{1.0}$ at 2 Torr and as $[A\ell]^{1.3}$ at 5 Torr when the Aℓ flow is varied by changing the Aℓ source temperature. The dependence of chemiluminescence intensity on [Aℓ] was also measured by changing [Aℓ] through *(i)* partially reacting Aℓ with O_2 upstream from the O-atom inlet, and *(ii)* changing the carrier Ar flow through the source while maintaining a constant Ar flow through the reaction tube. In those cases intensity dependences on [Aℓ] of 0.3 and 0.4, respectively, were observed at 5 Torr. The intensity of the glow upon O_2 addition decreased continuously, much faster than the decrease in [AℓO] calculated from the rate coefficient of the AℓO/O_2 reaction measured in the same reaction tube, suggesting that AℓO is not involved in the chemiluminescence. These facts and the high light yield observed point to a mechanism

$$X - A\ell + O \rightarrow A\ell O + X \qquad (6)$$

where X is, e.g., Aℓ. However, this conclusion is based on data which can only be regarded as preliminary. In further experiments it will be necessary to ascertain *(i)* that [O] does not change, or change differently, in the various experiments used to determine [Aℓ] dependence, *(ii)* proper mixing of reactants is achieved under all conditions, and *(iii)* O_2 impurities are not present in the carrier gas.

In experiments in which the N atoms were not titrated, and hence N rather than O atoms were present, a continuum of similar intensity to that of the Aℓ/O system was observed, which is, however, shifted to the blue. Since the $A\ell_2$/N reaction is only 2.0 eV exothermic, while the emission is found to extend to at least 287 nm (4.3 eV), an energy transfer mechanism appears indicated here. (While the Aℓ/N reaction could provide about 4.0 eV it appears an unlikely reaction for the same reasons as Reaction (2).) This in turn suggests that an energy transfer mechanism might also be considered for the Aℓ/O glow.

It should be pointed out that all of this work was done at a low $[A\ell] \approx 10^{11}$ ml^{-1}. Some discrete emissions were also observed for the Aℓ/O and N glows; their identification may have to await experiments at higher [Aℓ].

3. UV and VUV Photoabsorption and Photoionization Investigations – R.E. Huffman, AFGL (Work Unit 30).

During this period, a major part of the work of assessment of the spectroscopic requirements for computer codes of interest to DNA was carried out. Working meetings were held with W. Ali (NRL) and D. Hamlin (Science Applications) to learn more about the role of the ultraviolet fireball and associated cross sections in high-altitude nuclear bursts. Several predicted compositions of the ultraviolet fireball radiation were obtained and will be used to guide the wavelength regions of interest in future measurements. Much of this work was done in AFGL contractual association with PhotoMetrics, Inc.

4. UV and X-Ray Data for O_2 and O_3 – L.H. Weeks, A.C. Faire, AFGL (Work Unit 31).

Analysis of the ALADDIN 74 data was continued. Results on the molecular oxygen and ozone were 90 percent reduced. From 115 to about 140 km, the O_2, was typical of other summer midlatitude data, such as Krankowsky *et al* (1968). From 140 to 160 km, there was a very slight increase

above other quiet measurements which may reflect the effect of the slightly disturbed geomagnetic conditions present during ALADDIN 74. Analysis of the ALADDIN 74 ozone shows good agreement with Johnson *et al* (1952), also obtained for midlatitude summer conditions. It is believed that the spread in ozone data currently seen in publications reflects large systematic or random errors. Such uncertainties are not believed present in the UV absorption technique, partly because of the lower spread in data at midlatitudes. Error analysis suggests also inherent accuracy in this method, making it particularly useful for monitoring ozone variations due to disturbances such as aurora solar proton events and atmospheric nuclear tests.

Preliminary data analysis has been completed on falling sphere neutral density and temperature results that were acquired at Churchill Research Range, Canada on 10 April 1975 at 0954 hours UT under moderate geomagnetically disturbed conditions ($K_p \approx 5+$). Although the measurements were made in April near the onset of the spring transition, the data are in very good agreement with the normal winter (60°N January) models from the US Standard Atmosphere Supplements, 1966, except for minor structure details. Observations that are typical of either winter or spring conditions are not uncommon during this season of the year. Furthermore, the data tend to support an earlier analysis and tentative conclusion reported by Faire and Murphy which suggested that data obtained during quiet conditions may be associated with the cold model, while those acquired under disturbed conditions are more closely related to the normal model for 60°N January. Further analysis will be made to determine the effects of lower atmosphere dynamics and solar activity.

A rocketborne payload instrumented to make simultaneous measurements of optical absorption and falling sphere densities was successfully flown at Poker Flat Research Range, Alaska on 3 March 1976 in conjunction with the ICECAP 76 Program. Measurements of O_2, O_3 and total density were obtained with optical instrumentation by Weeks and falling sphere instrumentation by Faire. Excellent results were obtained during the peak of disturbed conditions resulting from an auroral breakup. Reduction of the data should provide density, temperature and composition results for use in analysis of the HIRIS data since the geophysical conditions were similar to those during the HIRIS launch. Another rocket flight on Feb 22, instrumented with just the optical instrumentation, provided reference data during quiet geomagnetic conditions. Data reduction and analysis is in progress.

5. *Recombination Rate, Energy Transfer to N_2 and O_2 from Vibrationally Excited NO^+—M. Camac, F. Bien, Aerodyne (Work Unit 32).*

Work has started on the determination of the vibrational lifetime of NO^+ (v = 1, 2 and 3) and the transfer of that vibration to N_2. The apparatus previously used in determining the absorption coefficient of NO^+ from the v = 1 to v = 2 vibrational levels has been modified in order to measure the vibrational transfer rate to N_2 and O_2. Work during this period has centered on making these modifications, together with recalibration of the tunable diode laser to tune over other vibration-rotation lines of interest.

The modifications of the NO^+ absorption cell include the addition of a gas-handling system to introduce N_2 and O_2 into the cell and a pressure-monitoring device to allow instantaneous measurement of gas pressure in the cell. Minor modifications were also performed on the ultraviolet lamps to insure more uniform UV discharge and to minimize the RF output when these lamps are discharged.

The tunable diode laser has been recalibrated. Due to the nature of this laser, the relative intensity of each lasing line changes with time. Thus, previously dominant laser lines have become weaker, while others, previously weak, now produce most of the laser emission intensity. The locations of the laser lines have not shifted, however. The dominant line is now located at 2319 cm^{-1} over a tuning current between 1.2 and 1.4 amperes as compared to 2323 cm^{-1} over the same current tuning range a year ago. This change allows the P-6 line of the v = 0 to v = 1 transition of NO^+ at 2319.9 cm^{-1}

to be measured in absorption. In addition, the R-1 line in the v = 1 to v = 2 vibrational transition at 2319.5 cm^{-1} as well as the R-11 line of the v = 2 to v = 3 absorption transition at 2319.1 cm^{-1} should be measurable.

The exact location of the laser light in the 2319 to 2320 cm^{-1} laser tuning range has been calibrated using CO_2 lines at 2319.175 cm^{-1} and at 2319.824 cm^{-1}. The position of the NO^+ vibration rotation transition from v = 0, 1 and 2 vibrational levels will be determined from the position of these CO_2 lines. The absorption of laser light as a function of time after the formation of NO^+ through photoionization would thus give the radiative lifetime and the relative formation rates of NO^+ in the three vibrational states.

6. *Reactions of Excited Atmospheric Gases—F. Kaufman, University of Pittsburgh (Work Unit 33).*

The rebuilt atomic line resonance absorption and fluorescence detection flow system is being used in a further study of the effective line shapes of O-atom resonance lamps. Laboratory experiments which had been performed in support of the ultraviolet absorption experiment on the Apollo-Soyuz Test Project had indicated high, effective Doppler temperatures for radio frequency ($\sim 10^8$ Hz) discharge lamps in pure He with a trace of added O_2. The latter is supplied by the simultaneous generation of O_2 from heated $KMnO_4$ and removal by an active getter (U or Ba). Surprisingly, this Doppler temperature was found to be substantially higher for r.f. than for microwave excitation in an otherwise identical lamp, i.e., $T_{r.f.} \approx 1100K$, $T_{\mu.w.} \approx 500$ K. Since one of the principal excitation mechanisms involves He metastables, the dissociative excitation is likely to populate high-lying states of atomic oxygen which reach the upper state of the resonance transition by a radiative and collisional cascade process. We are therefore studying the pressure dependence of the emitted line breadth over the range 1 to 20 Torr in order to verify the predicted narrowing with increasing pressure. The experiments involve the measurement of fractional absorption of unreversed OI triplets near 1300A (line ratios close to the theoretical 5:3:1) for different concentrations of O-atoms produced in the flow tube by the N + NO reaction. Early results suggest that the predicted pressure effect is qualitatively correct.

A large amount of work has gone into the performance and interpretation of laser-excited fluorescence lifetime experiments on NO_2 in the 6000A wavelength region. In that region there is strong evidence that the $^2B_2$ state is the only excited state which is reached in absorption. That state is, however, strongly perturbed by high vibrational levels of the ground state through vibronic coupling. The anomalously long radiative lifetime of NO_2 and the nonexponentiality of the radiative decays may then be explained as due to variable vibronic coupling. When strong vibronic features of the $^2B_2$ state are reached in absorption, biexponential decays with lifetimes of about 50 and 200 μsec, respectively, are observed. In between such features, the absorption is weaker, the decays are exponential, and the lifetime is long ($\sim$ 200 μsec). Furthermore, the total absorption band of NO_2 in the visible may be subdivided into its contributions by the $^2B_1$ and $^2B_2$ transitions on the basis of a variety of spectroscopic evidence, so that the integrated absorption coefficient due to the $^2B_2$ transition may be estimated independently. The corresponding lifetime of about 3 μsec, when multiplied by the appropriate level density ratio of about 10 leads to fair agreement with measured lifetimes of the stronger vibronic features of the fluorescence. Laser fluorescence experiments with narrow excitation and with moderate spectral resolution of the fluorescence are now underway. Particular care is taken not to introduce discrimination into the geometry of the field of view. The theory of Bixon and Jortner is being applied and may prove successful. The major lifetime anomaly of the stronger $^2B_1$ transition at shorter wavelength is still unresolved.

The infrared chemiluminescence experiments on the relaxation of HCl^v in v = 1 to 7, which is produced by the H + ClNO reaction, are going well. Quenching rate constants for specific v-states

by added ClNO reactant and by CO_2, N_2, or H_2 quenchers are being measured. ClNO is anomalously efficient, but this may be due, in part, to v-v interactions at the higher HCl^v concentrations which are attained with larger reactant densities. The values of k_{CO_2} increase from about 2×10^{-12} cm^3 sec^{-1} for v = 2 to 5×10^{-11} for v = 6. Much detailed information on relaxation processes now becomes available through efficient computer analysis of infrared chemiluminescence experiments in our fast-flow apparatus.

7. High Intensity Ion Source Data – J. Früchtenicht, TRW (Work Unit 34).

Investigations included (1) measurement of the relative concentrations of all ionic species that can result from the stopping of Al^+ ions in thick target gases composed of various admixtures of nitrogen and oxygen, and (2) conducting similar experiments with Fe^+ and Ti^+ ions.

The experimental phase of these measurements has been completed and analysis and interpretation of the data is in progress as is preparation of the final report.

The additional experiments tended to confirm the validity of the measurement technique in the sense that secondary and tertiary reactions were observed consistent with known rate constants. The basic conclusion is that Al^+ ions stop in the gas predominantly as neutral atoms remain. The same situation exists for Fe^+ and Ti^+ ions. The data are consistent with the dominance of charge exchange reactions during the stopping process. It was found during the course of these experiments that a significant fraction of the target gas molecular ions were produced by photoionization by photons emitted from the hot metal plasma at early times. This observation makes interpretation of the data a bit more difficult, but we believe that the bulk of the experimental evidence is consistent with the charge exchange thesis. These results will be discussed in detail in the final report.

D. Subtask L25BAX HX 632
"IR Phenomenology and Optical Code Data Base"

1. COCHISE – Ozone Investigations – J. Keneally, F. Del Greco, AFGL (Work Unit 03).

The COCHISE experimental facility has been almost fully operational for several months; both wavelength and radiometric calibrations have been carried out to assess capabilities of the infrared detection system, and some initial spectral observations have been made of chemi-excited radiation. Current overall system performance is consistent with the objectives established as design goals for the facility.

PART II – ABSTRACTS OF RELEVANT REPORTS

1. Experimental Measurement of NO^+ Radiative Lifetime – F. Bien, Aerodyne Research, Inc.

Report No. AFCRL-TR-75-0619
November 1975

The location and integrated absorption coefficient of the R-3 line for the v = 1 to v = 2 vibrational transition in NO^+ has been experimentally measured. The location of the line center was determined to be 2327.20 ± 0.01 cm^{-1}, 0.07 cm^{-1} higher than the previously calculated value. The line was found to be Doppler broadened, giving an integrated absorption coefficient of 240 ± (+100, −75) cm^{-2} atm^{-1}. This value would be consistent with a thermal equilibrium ground state integrated

absorption coefficient of 280 cm^{-2} atm^{-1}, one-half the value of previous observations and a factor of 3 higher than theoretical predictions. The accuracy in the ground state equilibrium value is ± a factor of 2 due to the uncertainty in relative vibrational populations.

2. *Fine Definition of IR Spectra from High Temperature Interactions of U + O_2 – Part II – D.W. Green, S.D. Gabelnick, G.T. Reedy, Argonne National Laboratory.*

Report No. DNA 3744F
August 1975

The reactions of UO and UO_2 with NO and NO_2 have been studied by infrared (IR) spectroscopy using the matrix-isolation technique. Codeposition of vaporized UO and UO_2 with NO_2 and with NO gases in an argon matrix at 14K resulted in the production of the UO_2^+ molecular ion with either a NO_2^- or NO^- anion. IR absorption frequencies have been measured and interpreted as the stretching modes of a linear UO_2^+ ion and a bent (bond angle = 109°) NO_2^- ion. Three different reactions have been observed to yield a UO_2^+ cation product: (1) UO_2 + NO_2; (2) UO_2 + NO; and (3) UO + NO_2.

3. *Experimental Photodissociation and/or Photodetachment of Atmospheric Negative Ions: Initial Results on O_2^- and CO_3^- – J.A. Vanderhoff, U.S. Army Ballistic Research Laboratories, and R.A. Beyer, NRC/BRL Research Associate.*

Report No. BRL MR 2594
February 1976

A drift tube mass spectrometer apparatus with a laser photon source has been constructed to measure photodissociation and/or photodetachment cross sections of atmospheric negative ions. Values for the cross sections of the negative ions of molecular oxygen and carbon trioxide are in good agreement with published results. Most of the data obtained for the discrete energies available to the Kr ion laser represent new results. These results reinforce the existing evidence of substantial structure in the spectrum of the negative carbon trioxide ion photodestruction cross section.

4. *Single and Double Clustering of Nitrogen to Li^+ – I.R. Gatland, School of Physics, Georgia Institute of Technology, Atlanta, and L.M. Colonna-Romano and G.E. Keller, U.S. Army Ballistic Research Laboratories.*

Report No. BRL-R-1858
February 1976

The clustering of nitrogen molecules to positive lithium ions has been studied experimentally using a drift tube. Two cluster ions were observed, a lithium ion with one attached nitrogen molecule and a lithium ion with two attached nitrogen molecules. The rate coefficients for the reactions which lead to the formation and destruction of these cluster ions have been measured as a function of the translational energy of the ions. The mobilities of positive ions of lithium and of the cluster ions drifting in nitrogen were also measured.

5. *New Atomic Beam Investigations at Low Energies – R.H. Neynaber, J.A. Rutherford, D.A. Vroom, Intelcom Rad Tech.*

Report No. DNA 3720F
October 1975

Final cross sections have been obtained for charge transfer between the ions O^+ and N^+ and the neutral atoms uranium and thorium. The processes studied can be represented as

$$O^+ + U \rightarrow O + U^+ \qquad O^+ + Th \rightarrow O + Th^+$$

$$N^+ + U \rightarrow N + U^+ \qquad N^+ + Th \rightarrow N + Th^+ \quad .$$

In the course of these measurements, cross sections were also obtained for the charge transfer reactions

$$CO_2^+ + U \rightarrow CO_2 + U^+ \qquad CO_2^+ + Th \rightarrow CO_2 + Th^+$$

$$N_2^+ + U \rightarrow N_2 + U^+ \qquad N_2^+ + Th \rightarrow N_2 + Th^+ \quad .$$

A second task completed was the measurement of cross sections for the reaction of $A\ell^+$ with molecular nitrogen and oxygen. Reactions for which cross sections were measured are

$$A\ell^+ + O_2 \rightarrow A\ell O^+ + O \qquad A\ell^+ + N_2 \rightarrow A\ell + N_2^+ \quad .$$

$$A\ell^+ + O_2 \rightarrow A\ell + O_2^+$$

Attempts were made to measure cross sections for other processes involving these reactants but no measurable signals could be detected. A final set of experiments involved a search for a route for formation of H_3O^+ using NO^+ as a precursor. No conclusive evidence for such a process could be found in the energy range covered by our experiments. During the course of these experiments cross sections were measured for the following reactions

$$N_2^+ + H_2O \rightarrow N_2H^+ + OH$$

$$N_2H^+ + H_2O \rightarrow H_3O^+ + N_2$$

$$N_2H^+ + O_2 \rightarrow O_2H^+ + N_2 \quad .$$

6. *Summary of Institute Proceedings: Magnetospheric Particles and Fields – B.M. McCormac, Lockheed Palo Alto Research Laboratory.*

Report No. DNA 3783F
September 1975

The presentations and discussions of the Summer Advanced Study Institute, "Magnetospheric Particles and Fields," held at Graz, Austria, August 4-15, 1975, are summarized.

7. *A Dynamic Model of the Neutral Thermosphere – K. Moe, M.M. Moe, McDonnell Douglas Astronautics Company.*

Report No. MDC G5891
September 1975

A dynamic model of the neutral atmospheric density for altitudes from 120 km to 450 km has been developed. It is a modification and extension of the preliminary model presented last year. The representations of the diurnal variation and the density bulges at low and high latitudes have been improved, and the semiannual effect has been introduced. A FORTRAN computer deck has been prepared. The density is expressed as a function of altitude, latitude, longitude, universal time, time of year, and the decimetric solar flux. It applies to the majority of days, when the geomagnetic planetary amplitude is between 5 and 20. The new model describes the global variations in density

more realistically than the static diffusion models commonly in use; yet its simple analytic form allows more rapid computation of densities. These characteristics make the model valuable both for operational use and for studies of atmospheric dynamics.

A mathematical representation of the spatial and temporal changes in density which occur during a geomagnetic storm has been developed. It has been used to construct a global model which is valid for all values of the geomagnetic planetary amplitude. A FORTRAN deck for this general model is in preparation.

A study of ionograms from the Alouette satellites has been initiated. The information these provide on the global properties of the ionosphere has important application to the energy sources, the composition, and the winds in the upper atmosphere.

8. Experimental Studies of Atomic Collision Processes Related to the Atmosphere – A.V. Phelps, U.S. National Bureau of Standards, Joint Institute for Laboratory Astrophysics.

Final Report
February 1976

A technique has been developed for the measurement of the rate coefficients for the electron excitation of molecular states of atmospheric interest. The technique was first applied to the ν_3 mode of CO_2 which radiates at 4.3 μm with a 2-msec lifetime. Measured electron excitation coefficients for the $b^1\Sigma_g^+$ state of O_2, which radiates at 762 nm with a 12-sec lifetime, are much smaller than expected and are being checked for systematic errors.

9. Charge Exchanges and Ion-Molecule Rearrangements in Disturbed E- and F-Regions (Implications for Optical Emissions and Deionization) – A.W. Ali, Naval Research Laboratory.

Report No. NRL MR 3165
November 1975

A comprehensive set of charge exchange and ion-molecule reactions are discussed. These reactions involve excited state species and arise in the disturbed E- and F-regions of the ionosphere. The reaction rates for most of these reactions are not known. However, some of them may play an important role in emission and deionization processes. These processes, therefore, can have important consequences for communications.

10. Atomic Beam Scattering Studies – B. Bederson, New York University, Department of Physics.

Final Report
July 1975

Work performed under Grant No. DA-ARO-D-31-124-73 G20 is described, for the period Aug 1, 1972-July 31, 1975. A summary of all measurements of electron-atom and electron-molecule cross sections performed under this grant is presented. This includes measurements of total and differential, elastic and inelastic cross sections with and without spin analysis, particularly of alkali metal atoms and molecules. A similar summary of polarizability measurements is also presented. Other activities of the laboratory, and a summary of personnel associated with the grant, are also presented.

11. Thermochemistry of Gaseous Metal Oxides – D.L. Hildenbrand, Stanford Research Institute.

Report No. AFGL-TR-76-0061
March 1976

The dissociation energies and ionization potentials of gaseous oxides in the Th-O, Zr-O, Ti-O, Eu-O, and U-O systems have been determined by high-temperature mass spectrometry. Dissociation

energies were derived from gaseous equilibrium measurements, while the ionization potentials were obtained from electron impact threshold measurements. Specifically, data were obtained for gaseous ThO, ThO_2, ZrO, ZrO_2, TiO, TiO_2, EuO, UO_2, and UO_3. Attempts to characterize the higher oxide of aluminum, $A\ell O_2$, were unsuccessful. New experimental information on the ionization potentials of Th, Zr, and Eu was also obtained. The results make it possible to accurately define the energetics of a number of ion-neutral and neutral-neutral reactions of the metals which are of importance in the analysis of nuclear burst effects.

12. *Investigation of Ion-Ion Recombination Cross Sections* — *D.L. Huestis, J.T. Moseley, D. Mukherjee, J.R. Peterson, F.T. Smith, and H.D. Zeman, Stanford Research Institute.*

Report No. AFCRL-TR-75-0606
November 1975

An experimental and theoretical investigation has been made of ion-ion mutual neutralization processes relevant to the chemistry of the D-region of the earth's ionosphere. This work is a continuation of earlier studies under Contract F19628-72-C-0121. In experimental work, the primary effort has been directed toward modifying the merged-beam apparatus, which had been designed to produce beams of small ions, so that it would produce hydrated ion beams of sufficiently high intensity and narrow energy spread. In the theoretical effort, our study of the ion-charged dipole interaction problem, which is being used as a model for the more complex interaction involving two clustered ions, has been continued. A classical dynamical study of this system in two dimensions using a fixed parabolic trajectory approximation and also a less accurate perturbation approximation has been completed. In order to extend this work to the case of three-dimensional motion, a powerful semiclassical perturbation technique, in which the collision S-matrix is expressible in closed form in terms of tabulated functions, has been developed. Using this approach preliminary calculations of orbital capture cross sections for the $O^- + NO^+$ system have been carried out. The uniform semiclassical S-matrix approach enables quantum effects such as interference and tunneling into classically nonallowed regions to be fully accounted for and comparison of semiclassical perturbation results with quantum mechanical close-coupling calculations for the e + CsF system has shown excellent agreement at all but the few smallest quantum numbers. A detailed study of the $NO_2^- \cdot H_2O$ system has been initiated in an effort to extend our approach from rotational excitation of diatomic molecules to the excitation of bending modes in simple hydrated ions.

13. *Calculation of Energetics of Selected Atmospheric Systems: Theoretical Study of Dissociative-Recombination of $e + NO^+$* — *H.H. Michels, United Technologies Research Center.*

Report No. AFCRL-TR-75-0509
September 1975

Calculations have been performed for the kinetics of the dissociative-recombination of an electron and the positive ion of nitric oxide. Electronic wavefunctions have been constructed for selected dissociating states of NO and expectation values of the electronic energy and electronic transition matrix elements have been calculated. The electronic wavefunctions for NO were analyzed to determine those states responsible for dissociative-recombination. States of $^2\Sigma^+$, $^2\Pi$, and $^2\Delta$ symmetry are found to be the most important channels for this reaction. Calculations are presented for the dissociation-recombination cross sections as a function of electron energy and vibrational state of the molecular ion. These data are also reduced to kinetic rate constants as a function of the electron temperature and ion vibrational temperature, assuming independent Boltzmann distribution functions. We find a calculated temperature dependence of $T_e^{-.39}$ for the rate coefficient with branching primarily into $N^2D + O^3P$.

AUTHOR–ORGANIZATION INDEX